P9.2 SUPERCOOLED CLOUD SCALE LENGTH AND CORRELATIVE RELATIONSHIPS

Charles C. Ryerson*, George G. Koenig, Constance L. Scott, Eric V. Phetteplace
Cold Regions Research and Engineering Laboratory, Hanover, New Hampshire

1. INTRODUCTION

The spatial variability of cloud microphysical properties is critical to understanding cloud properties and their interaction with the environment. Understanding the spatial variability of cloud microphysical properties is especially important in supercooled clouds that cause airframe icing. The utility of aircraft icing forecasts, as suggested by Politovich (1999), is dependent upon the ability to analyze and depict the expected variability of cloud properties in a forecast area. That is, highly variable icing conditions are more difficult to predict and have less predictable effects on aircraft performance than less variable conditions. Forecasts that cannot predict or convey the potential variability of conditions are less useful to pilots.

In this paper we characterize the spatial properties of supercooled cloud liquid water content (LWC) using variations of cluster analysis and thresholding methods for clouds measured in the NASA Supercooled Large Drop Research Program (SLDRP) conducted in the late 1990s (Miller et al., 1998). We also briefly assess correlative relationships between liquid water content and other cloud properties that may be used to indicate the variability of LWC. Our analyses are intended to indicate how much cloud LWC varies spatially in supercooled clouds. Since all measurements in a flight are not made simultaneously, we are actually assessing spatial/temporal variations. We do not attempt to create a climatology of LWC variability because we have analyzed only one winter of measurements in a small region. Our intent is to demonstrate several methods of assessing LWC variability with the intent of using at least one of the methods for later, more extensive, climatological analyses.

* *Corresponding author address:* Charles C. Ryerson, U.S. Army Corps of Engineers, Engineer Research and Development Center, Cold Regions Research and Engineering Laboratory, 72 Lyme Road, Hanover, NH 03755-1290; email: charles.c.ryerson@erdc.usace.army.mil

2. BACKGROUND

The accuracy of icing forcasts and the impact of icing on aircraft performance are related to the spatial fluctuation of microphysical properties within the clouds. Fluctuation of LWC can seriously affect aircraft performance by driving icing conditions above and below the Ludlam limit. Though a forecast may have indicated moderate icing conditions, for example, actual cloud conditions may consist of overall supercooled LWC in the moderate icing range punctuated by peaks of high LWC – perhaps above the Ludlam limit. These spikes could drive icing from dry growth, rime, to wet growth, or clear icing, that has a different and potentially more dangerous impact on aircraft performance (Koenig, et al., 2003). An ability to probabilistically characterize fluctuations of LWC within forecasts could have a significant impact on the prediction of icing forecast severity.

In attempts to develop methods for characterizing the fluctuation of icing cloud microphysical conditions, Jameson and Kostinski (2000) and Ryerson et al., (2001, 2002) investigated various methods. Jameson and Kostinski (2000), for example, have developed a cluster analysis technique that relies on characterizing the changes of elements of the drop size spectra with time. They have also applied this method to hypothetical icing cloud LWC series with varying magnitudes of clustering. Ryerson et al. (2001) addressed characterization of clustering in NASA flight data, some of which is used in this report, for assessing the fluctuation of LWC within clouds, especially with regard to potential influence on remotely sensed LWC. Koenig et al. (2003) have also simulated the effect of fluctuating icing conditions on actual ice shapes formed in an icing wind tunnel.

3. CLOUD MICROPHYSICS

LWC measurements were made by the NASA Glenn Research Center's (NASA-GRC) Twin Otter research aircraft during the SLDRP conducted from the Fall of 1996 to December 1999 (Miller et al., 1998). SLDRP was a joint NASA, National Center for Atmospheric Research

(NCAR), and FAA program with an objective to acquire a supercooled large drop (SLD) database for characterization of the SLD environment, freezing drizzle and freezing rain, aloft.

Based on specilaized forecasts and real-time inflight guidance provided by NCAR, the NASA-GRC Otter was flown from Cleveland, Ohio to locations where conditions were believed to be conducive to finding SLD aloft. Flights were conducted over regions adjacent to Lake Erie and Lake Michigan extending as far south as Parkersburg, West Virginia. Though SLD were often located, large portions of most flights encountered no SLD, especially when in transit to or from an area with forecasted SLD.

LWC measurements used in this study were obtained from a King hot wire probe mounted on the Otter's nose. The probe has a measurement range of 0-1.0 gm^{-3}, and liquid water is supplied as 1-s measurements. Probe zero offset was adjusted by comparing King probe mean LWC during a flight segment against a Forward Scattering Spectrometer Probe (FSSP) mean LWC for the same period. The King probe zero-offset was adjusted to allow King and FSSP mean LWCs to match as closely as possible while maintaining non-negative LWC values from the King probe.

This report uses SLDRP data from 17 flight segments extracted from 14 flights during the winter of 1997-1998. Dependence of LWC variability on height above cloud base (or below cloud top), temperature, and turbulence led us to seek flight segments that, as much as possible, occurred at a nearly constant altitude. We used flight segments with varying heading to lengthen our flight segments for better statistics with the assumption that cloud conditions were generally isotropic directionally. Cloud particle images were inspected using a 2-D gray Optical Array Probe to characterize flights as pure liquid, mixed phase, or fully glaciated. Insufficient information was available to exclude turbulence effects. Flights selected for analysis had no breaks in cloud.

4. CLUSTERING AND STATISTICAL SIMILARITY

Clustering of supercooled LWC values associated with patchy clouds (Jameson and Kostinski, 2000) can increase the potential for dangerous in flight icing conditions relative to clouds that do not exhibit patchiness but have the same total LWC. Clustering of supercooled LWC increases the probability of exceeding the Schumann-Ludlam limit, thus increasing the probability that a high value of LWC will be followed by another high value of LWC rather than a low value. To explore clustering of LWC we analyzed three flights from the NASA SLDRP program in 1998 (Miller et al., 1998) using the 1-s LWC measurements and segment lengths of 10, 30 and 90-s to compute three statistical moments; the average (μ), standard deviation (σ), and skewness(*s*) of the LWC values associated with each segment. Next, we determined if consecutive segments were statistically similar based on the computed moments. This process was repeated and consecutive statistically similar segments were grouped together to form a cluster. We used different segment lengths to gain insight on the impact of scaling on the cluster analysis.

Before analyzing the time series to determine clusters, we computed the average, standard deviation, variance, skewness, range of values, coherence length, and cluster intensity for the entire flight series to understand the LWC conditions along the flight path. We used a two-point correlation algorithm (Kostinski and Jameson, 1997) to compute the coherence length and defined the cluster intensity as being proportional to the global standard deviation.

$$\aleph \propto \sigma \tag{1}$$

Both the coherence length and the statistical moments differ significantly from flight to flight.

The deviation of the normalized distribution of the measured LWC values from the corresponding standard normal distribution reflects the potential for clustering. The normalized distribution of LWC has a mean of zero based on

$$lwc_i' = lwc_i - \mu \tag{2}$$

Figure 1 compares the distribution of lwc_i' against a standard normal distribution with the same standard deviation for flight 980224f1b.

The normalized distribution of the measured LWC values differ from the computed standard normal distribution for both large (0.28-0.34 g/m^3) and small (-0.06 to -0.12 g/m^3) deviation. As noted, deviations from a standard normal distribution imply an increased potential for clustering. Similar results were found for the other two flights analyzed, supporting the concept of clustering.

To explore the clustering of the LWC values we divided the time series into segments of equal

duration and computed the local average, standard deviation, and skewness for each segment. The number of segments N_s for a time series of N one-second measurements with segment lengths of n_s and a moving average of n_s equals

$$N_s = N - 2n_s \quad (3)$$

For each segment we calculated the average, μ_s^i, the standard deviation, σ_s^i, and the skewness, s_s^i. Next, we calculated the change in each of the statistical moments for consecutive segments ($m_1^i = \mu_s^{i+1} - \mu_s^i$, $m_2^i = \sigma_s^{i+1} - \sigma_s^i$, and $m_3^i = s_s^{i+1} - s_s^i$). If the difference satisfies the following criteria

$$m_j^i \le 0.05 * \left[\max\left(m_j^i\right) - \min\left(m_j^i\right) \right] \quad (4)$$

Table 1. Statistical moments and derived parameters for three LWC flight series.

Moment/Derived Parameter	Flight 980302f1	Flight 980224f1b	Flight 980212f1
Flight duration (seconds)	1462	793	1702
Average (g/m^3)	0.045	0.141	0.202
Maximum LWC (g/m^3)	0.343	0.497	0.379
Minimum LWC (g/m^3)	0.001	0.001	0.003
Standard Deviation (g/m^3)	0.060	0.129	0.085
Variance (g/m^3)	0.003	0.017	0.007
Coherence length (seconds)	9	105	584
Cluster Intensity	$\propto$ 0.06	$\propto$ 0.129	$\propto$ 0.085

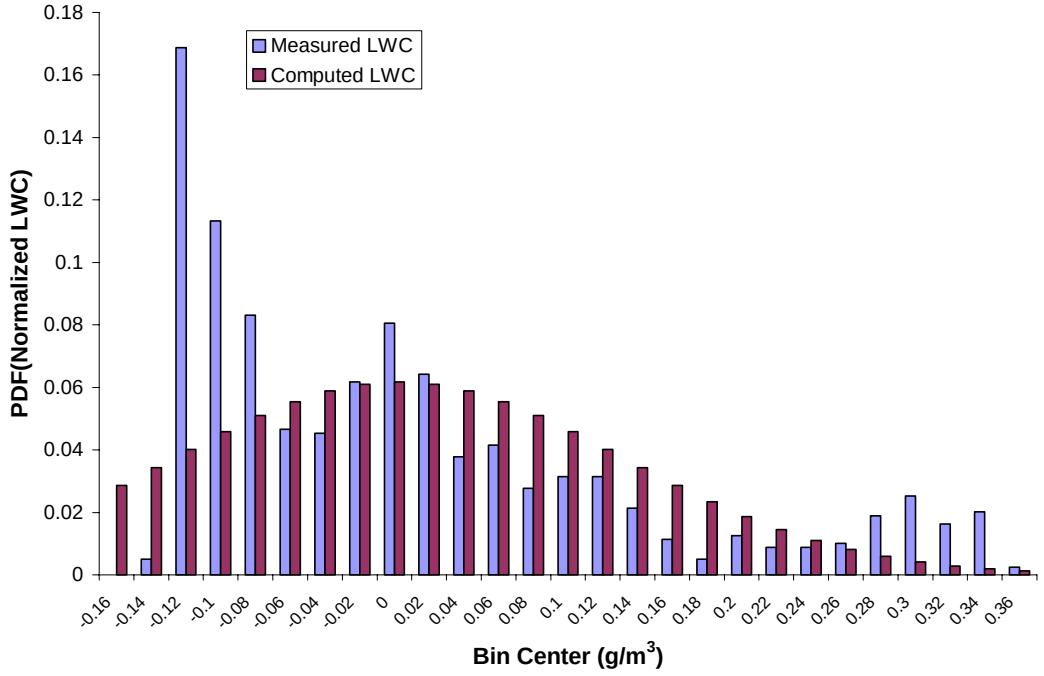

Figure 1. Comparison of the normalized measured LWC distribution and the computed standard normal distribution with the same standard deviation as the measured values for flight segment 980224f1b.

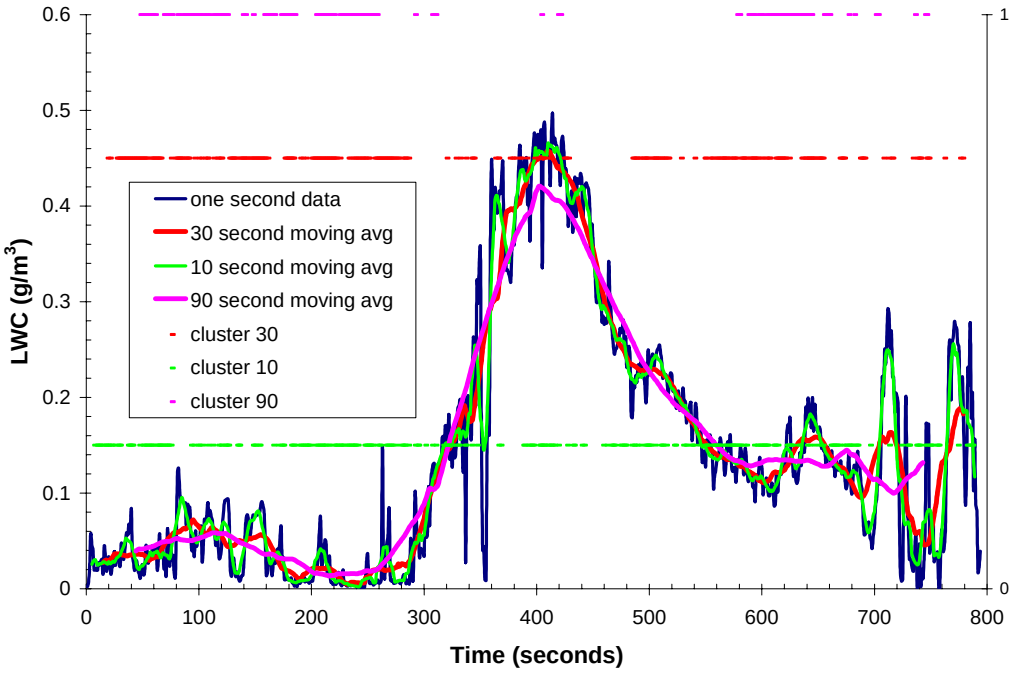

Figure 2a. Clusters determined using segment lengths of 10, 30, and 90-s for flight segment 980224f1b.

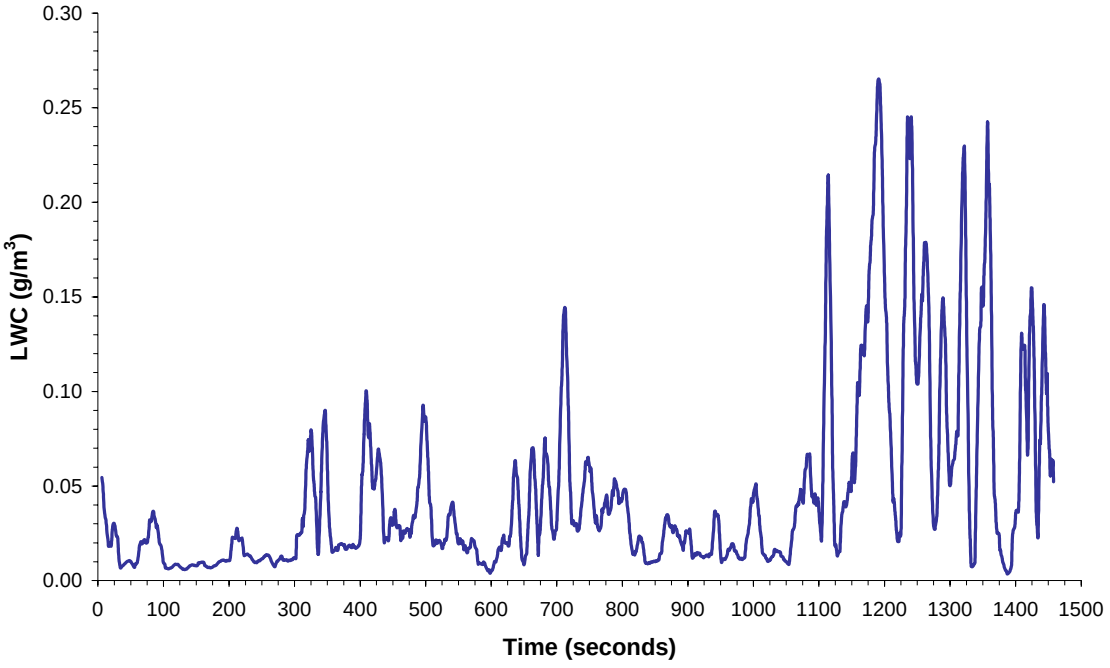

Figure 2b. Ten second moving average of the LWC values for flight segment 980302f1.

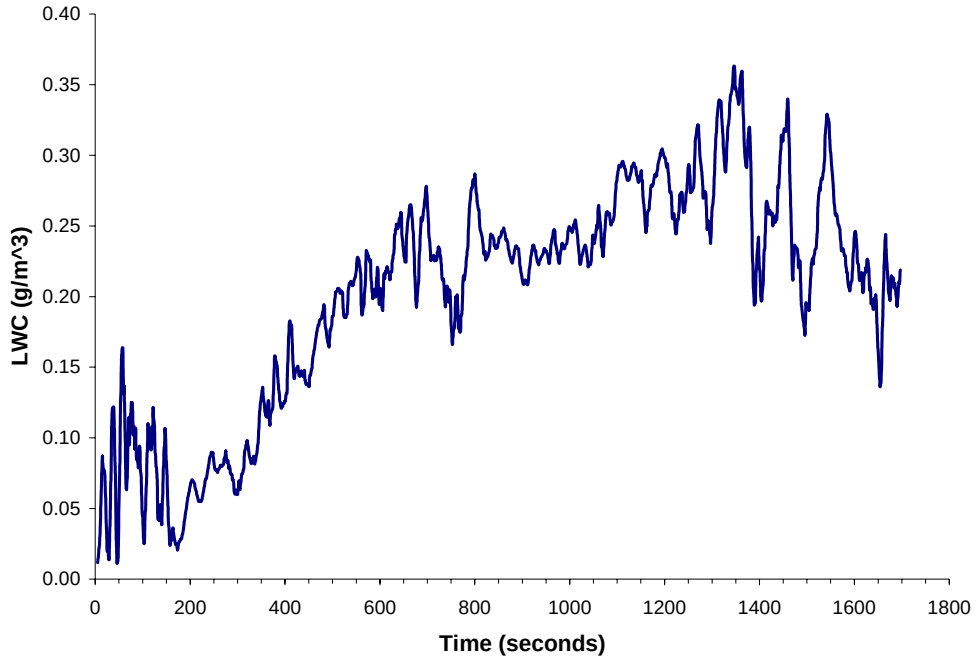

Figure 2c. Ten second moving average of the LWC values for flight segment 980212f1.

Table 2. Cluster/gap characteristic as a function of Cluster Intensity (CI) and coherence length (CL).

	# of cluster Segments / # of gap segments	Max Cluster Length (segments)	Max Gap Length (segments)
Flight 980212f1 CL=584 STDEV=0.085	1.009	11	23
Flight 980224f1b CL=105 STDEV=0.129	0.543	9	20
Flight 980302f1 CL=9 STDEV=0.060	0.949	14	23

the segments *i*+1 and *i* were flagged as being statistically similar for statistical moment *j*. The process continues until the entire time series is processed. In the final step, we combine consecutive segments to form clusters by requiring that each statistical moment for the segment meets the criteria given in Equation 4. We used segment lengths of 10, 30, and 90-s to explore the impact of the segment size on clustering. As the segment length increases larger gaps or regions occur where one or all of the statistical moments fail the inequality in Equation 4. Both the standard deviation and the skewness associated with the 90-s segments in flight 980224f1b are less than the values for the 30 and 10-s segments. The larger gaps, as seen in Figure 2a, associated with the 90-s segments result from the failure of the changes in the average LWC of consecutive segments to meet the criteria set forth in Equation 4. A close inspection of Figure 2a in the region from 250 and 600 seconds reveals why. The average of the 90 second segments in this region are either increasing or decreasing monotonically. Thus, the change in the average for consecutive segments fails Equation 4. Clustering determined in this fashion depends on the size of the segment used in the analysis. This is a common theme in dealing with the determination of clusters associated with a time/space series of measurements of LWC or cloud drop concentrations. What is the appropriate scale to use to analyze a time series of LWC values?

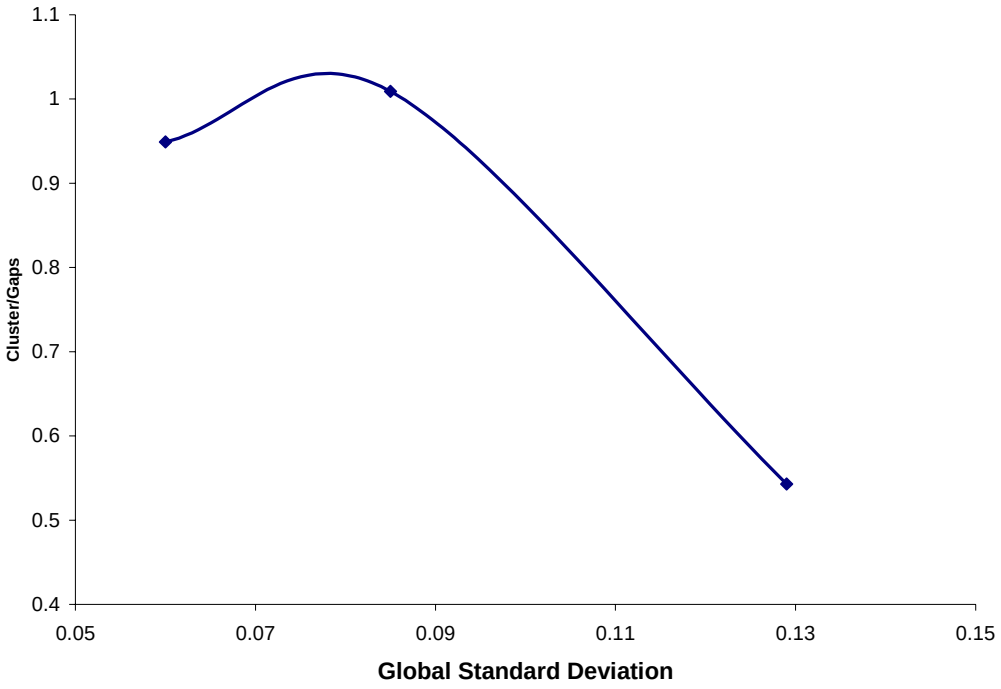

Figure 3. The ratio of the number of cluster segments to the number of gap segments as a function of the global standard deviation.

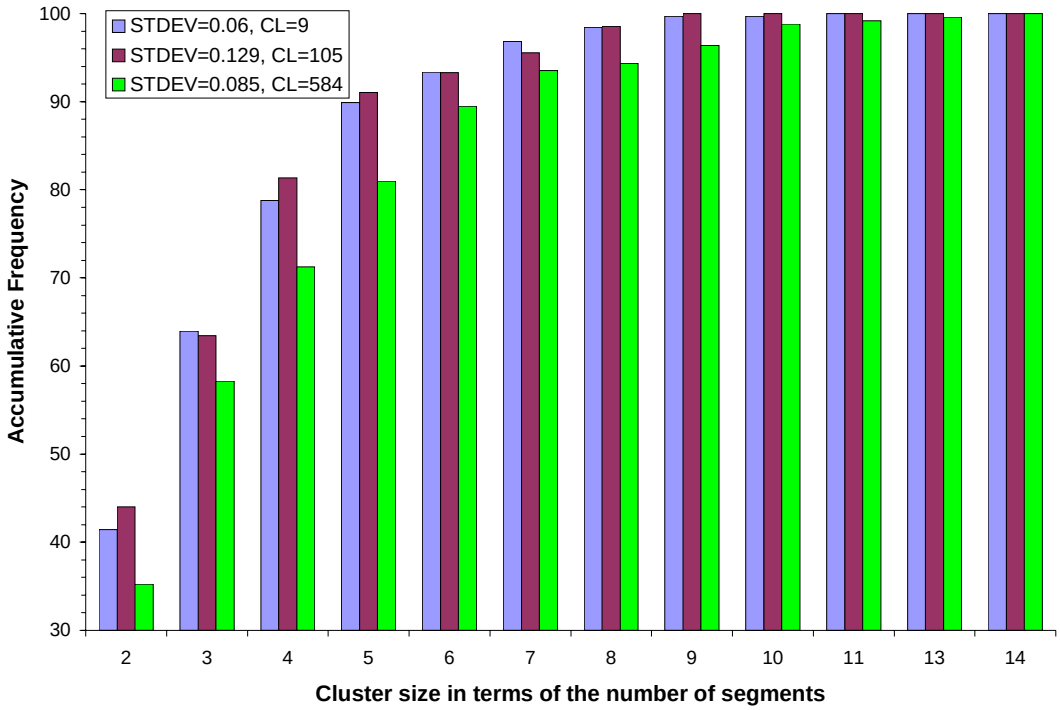

Figure 4. The frequency of occurrence of cluster lengths with the indicated number of segments. Blue bars are flight segment 980302f1, maroon bars are flight segment 980224f1b, and green bars flight segment 980212f1.

Table 3. Flight LWC characteristics based on the entire data series.

flight	Average LWC (μ) (g/m^3)	Skewness (g/m^3)	Standard Deviation (g/m^3)	Number of 1-second data points	Coherence Length (1-sec pts)	Maximum LWC (g/m^3)
980112f1	0.105	0.7606	0.0723	985	41	0.3242
980126f2	0.124	0.9073	0.0917	2584	82	0.4845
980126f3	0.164	1.7963	0.15570	1560	109	0.6846
980130f1	0.086	0.3145	0.05706	1362	49	0.2256
980204f1a	0.030	1.1364	0.00759	2536	9	0.0723
980204f1b	0.195	2.6225	0.08977	2668	12	1.4135
980204f2	0.218	1.6539	0.46704	5165	232	1.4018
980204f3	0.054	0.3316	0.03103	726	242	0.1418
980205f1	0.092	2.2077	0.05993	1791	71	0.6355
980205f2	0.018	1.7165	0.00936	909	12	0.0702
980212f1	0.201	-0.6269	0.08543	1703	12	0.3793
980224f1b	0.140	1.0693	0.12916	704	104	0.497
980224f1bb	0.095	1.0264	0.08797	1873	44	0.4248
980227f1	0.271	1.8164	0.20784	2401	26	1.3154
980302f1	0.045	2.4641	0.06034	1462	9	0.3433
980318f1a	0.042	5.3522	0.03991	1186	23	0.4589
980318f1b	0.095	1.02649	0.08797	1873	44	0.4248

As indicated in Table 1 the coherence length and standard deviation differ from flight to flight. We explored the relationship of clustering for the different flights using a segment length of 10-s, dictated in part by the short coherence length associated with flight 980302f1. In general, we want to use a segment length less than or equal to the coherence length determined from the two point correlation algorithm.

Using a segment length of 10-s, we explored the clustering/gap characteristics of three flights with different LWC characteristics as evident in Table 1. Clusters represent regions of statistical continuity as defined by Equation 4, while gaps are regions where consecutive segments fail the inequality. The ratio in column 2, Table 2 represents the number of segments flagged as clusters based on the inequality in Equation 4 divided by the number of segments that failed (gap segments) the inequality. While the data set used in the analysis consists of only three flights, Figure 3 indicates a relationship exists between the cluster/gap ratio and the global standard deviation. We plan to analyze the rest of the flight information we have in a similar manner. Figure 4 presents the distribution of cluster lengths as a

Flight 980224f1b, with the highest value of the standard deviation, also has the highest frequency of occurrences of clusters with segment lengths of 2, 3, and 4 segments, while flight 980212f1 with a long coherence length has the lowest frequency of clusters. While there is little change in the accumulative frequency for flight 980224f1b and flight 980302f1 for clusters consisting of more than eight segments, the accumulative frequency continues to change for flight 980212f1 reflecting the fact that flight 980212f1 has clusters with larger segment counts consistent with the larger coherence length. Defining clusters based on statistical continuity between consecutive segments depends on the segment size and each of the statistical moments.

Additional data analysis of flight data needs to be accomplished to fully explore the utility of this approach. However, since the focus is on aircraft icing we also explored the use of threshold techniques to determine the duration and frequency an aircraft would be in LWC conditions that exceed a specified threshold. Rather than use values like the Schumann-Ludlam limit or the values for trace, light, moderate, and severe icing (Politovich, 1999), we set our threshold relative to the global average for the flight data being analyzed.

Table 4a. Computed characteristics for each flight based on a threshold (*T*) defined as 1.25*average LWC. ALWC= Accumulative LWC and TLWC = total LWC for the flight.

Flight	Percent of 1-s pts $LWC \geq T$ (%)	Percent of 1-s pts $LWC < T$ (%)	$\frac{LWC \geq T}{LWC < T}$	$ALWC \geq T$ (g/m^3)	$\frac{ALWC \geq T}{TLWC}$ (%)
980112f1	30.0	69.9	0.430	58.6	56.29
980126f2	29.5	70.4	0.419	187.0	58.19
980126f3	24.2	75.7	0.320	256.2	32.22
980130f1	35.5	64.4	0.551	73.2	62.26
980204f1a	13.0	86.9	0.150	14.6	19.22
980204f1b	20.8	79.2	0.263	178.9	34.37
980204f2	27.7	72.2	0.384	547.7	48.62
980204f3	32.7	67.2	0.488	21.6	55.00
980205f1	23.5	76.4	0.308	75.3	45.27
980205f2	21.0	78.9	0.266	6.1	36.95
980212f1	29.3	70.7	0.414	143.8	42.00
980224f1b	30.2	69.7	0.433	73.2	65.56
980224f1bb	32.7	67.2	0.488	123.7	69.51
980227f1	28.6	71.3	0.401	366.5	56.16
980302f1	22.5	77.5	0.290	44.3	66.88
980318f1a	18.5	81.4	0.228	20.4	40.36
980318f1b	32.7	67.2	0.488	123.7	69.51

Table 4b. Additional characteristics of flights based upon threshold *T*.

Flight	$ALWC < T$ (g/m^3)	$\frac{ALWC < T}{TLWC}$ (%)	$\frac{ALWC \geq T}{ALWC < T}$
980112f1	45.5	43.71	1.288
980126f2	134.9	41.81	1.392
980126f3	539.0	67.78	0.475
980130f1	44.4	37.74	1.650
980204f1a	61.6	80.78	0.238
980204f1b	341.7	65.63	0.524
980204f2	578.9	51.38	0.946
980204f3	17.6	45.00	1.222
980205f1	91.0	54.73	0.827
980205f2	10.4	63.05	0.586
980212f1	198.	58.00	0.724
980224f1b	38.4	34.44	1.904
980224f1bb	54.2	30.49	2.280
980227f1	286.2	43.84	1.281
980302f1	21.9	33.12	2.019
980318f1a	30.2	59.64	0.677
980318f1b	123.7	30.49	2.280

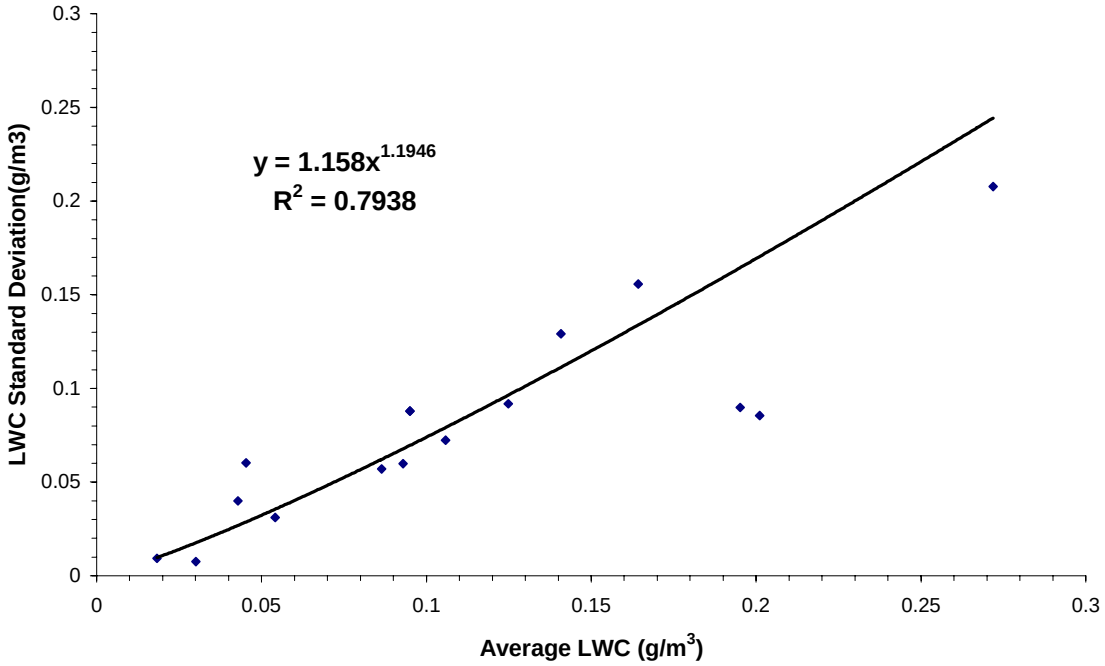

Figure 5. Scatter diagram of the average LWC vs. the LWC standard deviation for each flight.

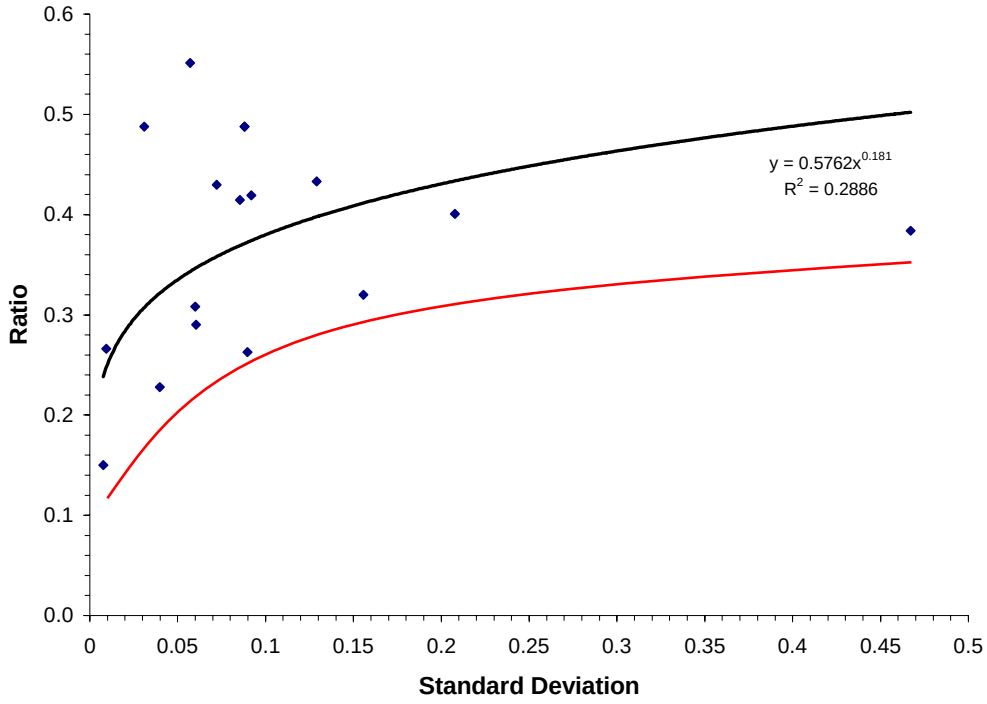

Figure 6. Scatter diagram of the standard deviation vs. $LWC \geq T$ / $LWC < T$

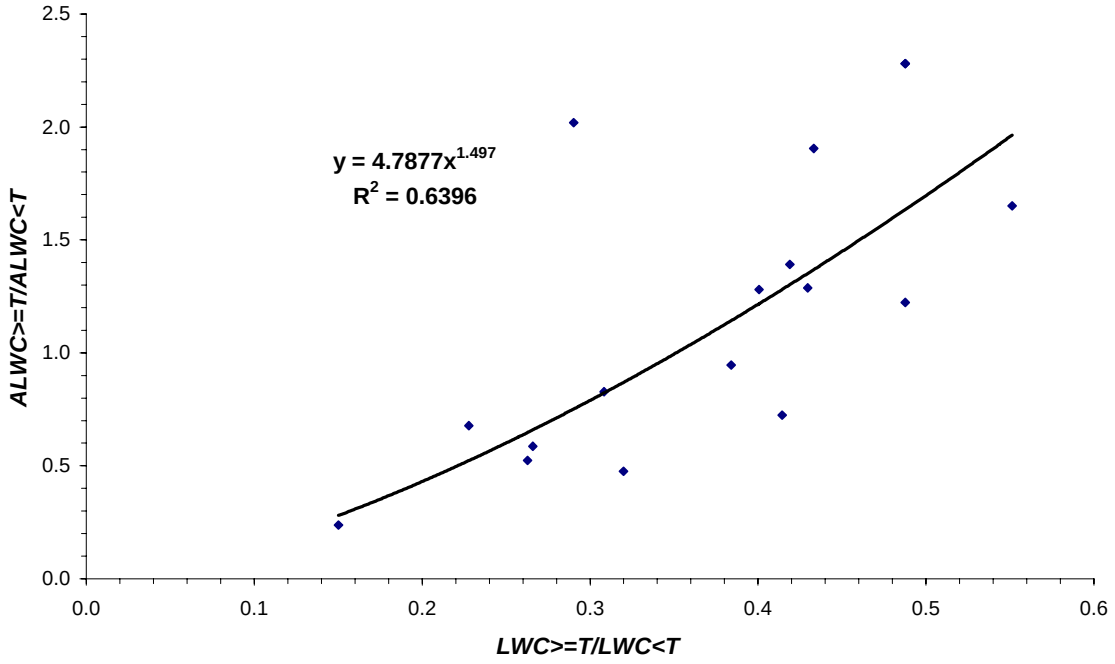

Figure 7. Scatter diagram of $LWC \geq T / LWC < T$ vs. $ALWC \geq T / ALWC < T$

5. LWC ANALYSIS BASED ON RELATIVE THRESHOLD

In this section, we explore horizontal variability of LWC for a number of flight series by defining a threshold relative to the average LWC for the flight. The selected threshold used was 1.25 times the average value. For each flight, we determine the points that satisfied the following criteria;

$$pts \geq 1.25 * \mu \quad and \; pts < 1.25 * \mu \qquad (5)$$

We also determine a number of parameters (Table 3) based on the data series.

The coherence length, based on a two-point correlation algorithm, represents the 'average' distance in terms of 1-s data points where the value of the correlation first drops to a value of 1/*e*. Columns 2 and 3 in Table 4a represent the percent of LWC measurements meeting the criteria given in the header row of the column. The total number of points associated with each flight can be found in Table 3 column 5. The rest of the columns are self-explanatory.

Some interesting results appear in the information contained in Tables 4a and 4b. For example, for flight 980112f1, while only 30% of the points meet the criteria $LWC \geq T$ these points account for 56.29% of the TLWC. The ratio of $LWC \geq T / LWC < T$ never even comes close to approaching one, in fact the largest value is 0.55, while the ratio $ALWC \geq T / ALWC < T$ ranges from a low of 0.238 to a high of 2.280. Ratios greater than one indicate there are more points or more ALWC associated with points meeting the $LWC \geq T$ criteria than points meeting the $LWC < T$ criteria. To explore the information contained in this dataset we plotted a number of scatter diagrams looking for relationships, or clustering of information, for the various parameters in Tables 4a and 4b. For all of the 17 flight segments the average LWC increases as the standard deviation increases. A power law provided the best fit to the data (Figure 5). If we know the average LWC or can predict the average LWC, we can use the relationship given in Figure 5 to provide an estimate of the standard deviation. However, this relationship applies only to the flights we analyzed.

In Figure 6, the scatter diagram relates the standard deviation to the ratio of the points computed using the criteria $LWC \geq T / LWC < T$. While the correlation coefficient is relatively low, as the standard deviation increases the ratio increases and none of the ratios fall below the red line in

Figure 6. Figure 7 is a scatter diagram of $LWC \geq T / LWC < T$ vs. $ALWC \geq T / ALWC < T$. The r^2 for this relationship is 0.63, the correlation coefficient is 0.79, and a power law provides the best fit.

The next series of figures represent the LWC series for three flights along the curve in Figure 7. Figure 8a represents flight 980204f1a with a $LWC \geq T / LWC < T$ =0.15 and $ALWC \geq T / ALWC < T$ =0.238. This point is located at the lower end of the curve in Figure 7. The magenta line at the top of the figure represents the points meeting the criteria $LWC \geq T$, while the magenta line at the bottom represents points meeting the criteria *LWC<T*. The black horizontal line represents *T=1.25*average LWC* for the series.

The histogram in Figure 8b gives the percentage of intervals with lengths defined in terms of 1-s points indicated by the x-axis values and the percentage ALWC falling in the indicated bin lengths. That is, the percentage of intervals for bin length *i* equals

$$\textit{Percentage of intervals for bin } i = \frac{\textit{number of intervals of length } i}{\textit{total number of intervals for } LWC \geq T} \quad (6)$$

While the percentage of the accumulative LWC for bin *i* equals

$$\textit{Percentage of ALWC for bin length } i = \frac{\textit{ALWC for all bins of length } i}{\textit{total ALWC for } LWC \geq T} \quad (7)$$

In Figure 8b 76% of all the points meeting the criteria of $LWC \geq T$ fall in a bin length of one and account for 40% of the accumulated LWC.

Figure 9a represents flight 980204f2 with a $LWC \geq T / LWC < T$ =0.384 and $ALWC \geq T / ALWC < T$ =0.946. This point is located in the middle of the curve in Figure 7. For flight 980204f2 we have a decrease of approximately 15% of single point bin lengths (72% to 58%) and a decrease of the ALWC from approximately 40% to 16% for the single point bin lengths relative to the values for flight 980204f1a. However, flight 980204f2 has bin lengths as large as 42 consecutive 1-s points, while flight 980204f1a's longest bin length is 14.

Figure 10a represents flight 980130f1 with $LWC \geq T / LWC < T$ =0.551 and $ALWC \geq T / ALWC < T$ =1.65. This point is located at the upper end of the curve in Figure 7. For flight 980130f1, we have intervals as long as 116 consecutive 1-second points and approximately 27% of the ALWC for points meeting the criteria of $LWC \geq T$ fall in this interval.

We can make some general statements relative to the dataset from the above analyses. As the average LWC increases the standard deviation increases. In addition, as the ratio of $LWC \geq T / LWC < T$ increases then $ALWC \geq T / ALWC < T$ increases and we encounter longer intervals with the LWC greater than or equal to *1.25*average LWC.*

6. CORRELATIVE RELATIONSHIPS

The seventeen flight segments described above were used to assess correlative relationships among cloud variables. The intent, as indicated earlier, was to allow estimation of LWC variance based upon other cloud characteristics as suggested by Politovich (1999).

Correlations between LWC and other cloud variables were made using measurements at 1-s intervals. However, a 5-s running mean was applied to all measurements to reduce rapid fluctuations that could, in part, be instrument induced and that might hinder identification of relationships because of the different response times of instruments and cloud microphysics. Typical aircraft speed was about 70 m s^{-1} making the spatial averaging about 350 m. We related the following variables to LWC; median volume drop diameter (MVD: microns), total temperature (TT: ºC), static temperature (ST: ºC), dew point temperature (DP: ºC), altitude (ALT: m above msl), and FSSP particle concentration (particles/m^3).

Overall, relationships between LWC and the other variables are weak, with r^2 being typically less than 0.7 (Table 5). In general, r^2 varied considerably among flight segments for LWC

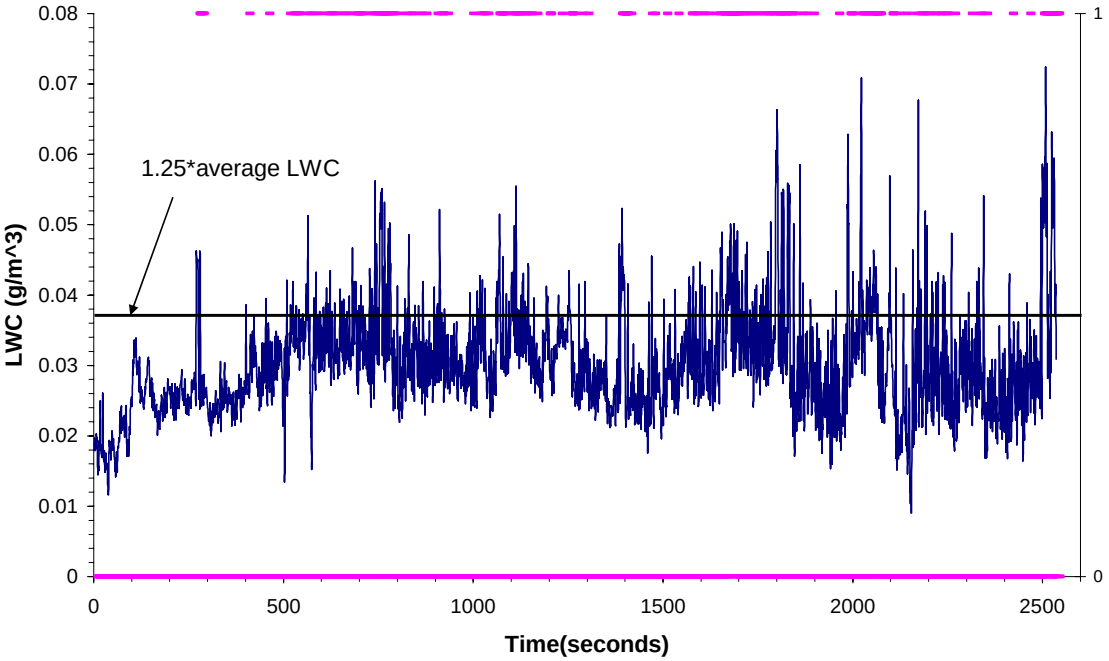

Figure 8a. Magenta lines represent LWC greater or equal to the threshold or less than the threshold for flight segment 980204f1a. See text for additional explanation.

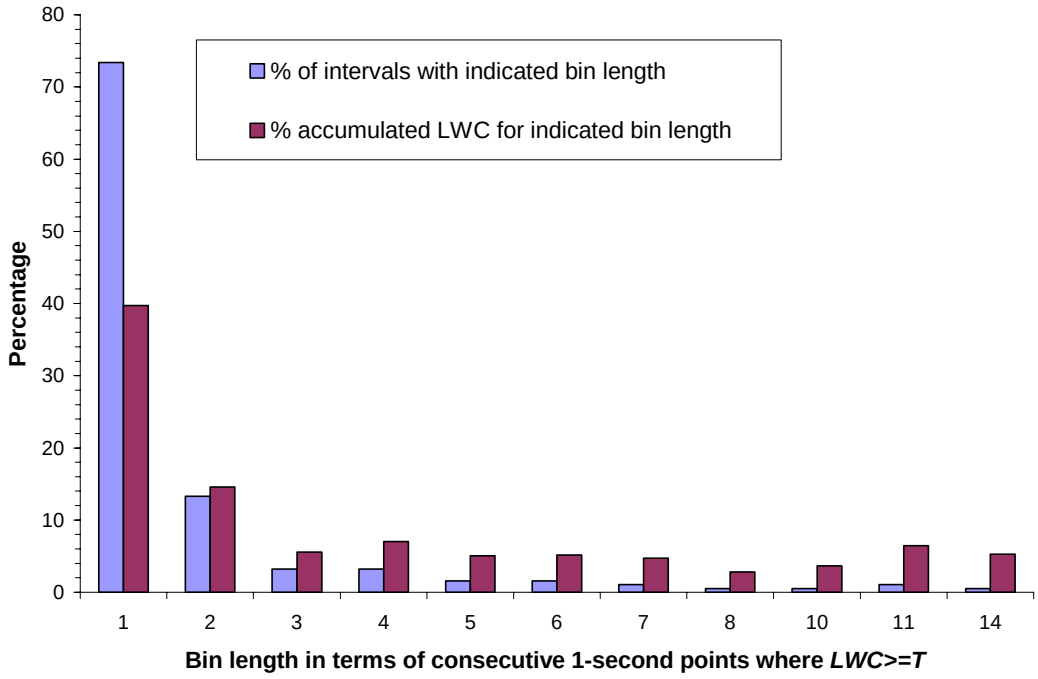

Figure 8b. Percentages of intervals and accumulated LWC by bin length for flight segment 980204f1a.

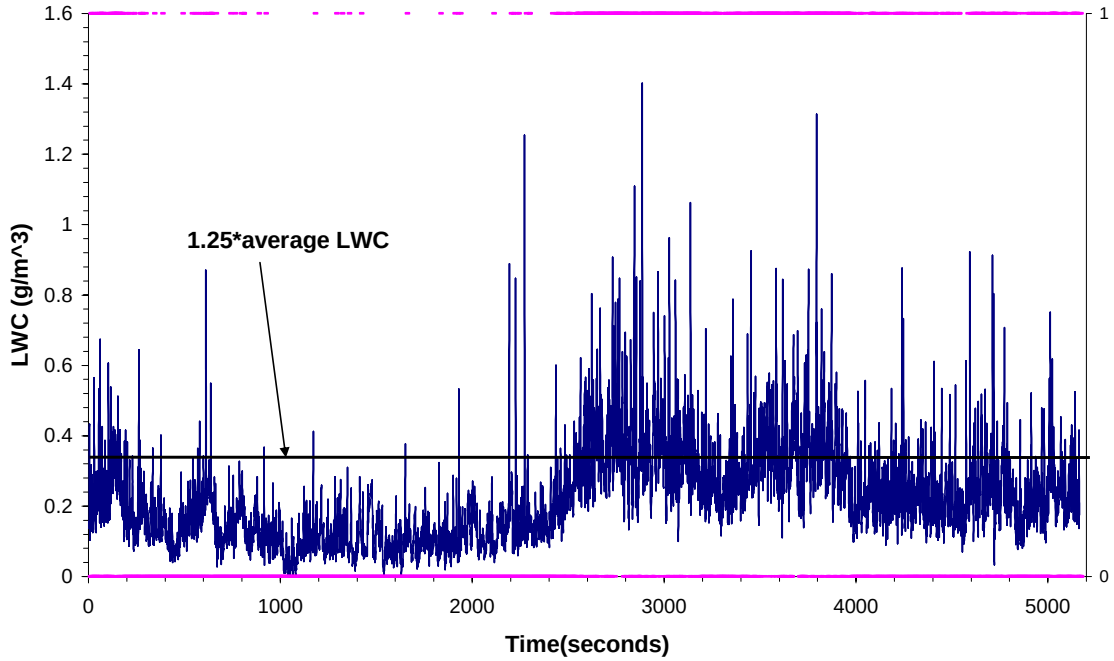

Figure 9a. Magenta lines represent LWC greater or equal to the threshold or less than the threshold for flight segment 980204f2. See text for additional explanation.

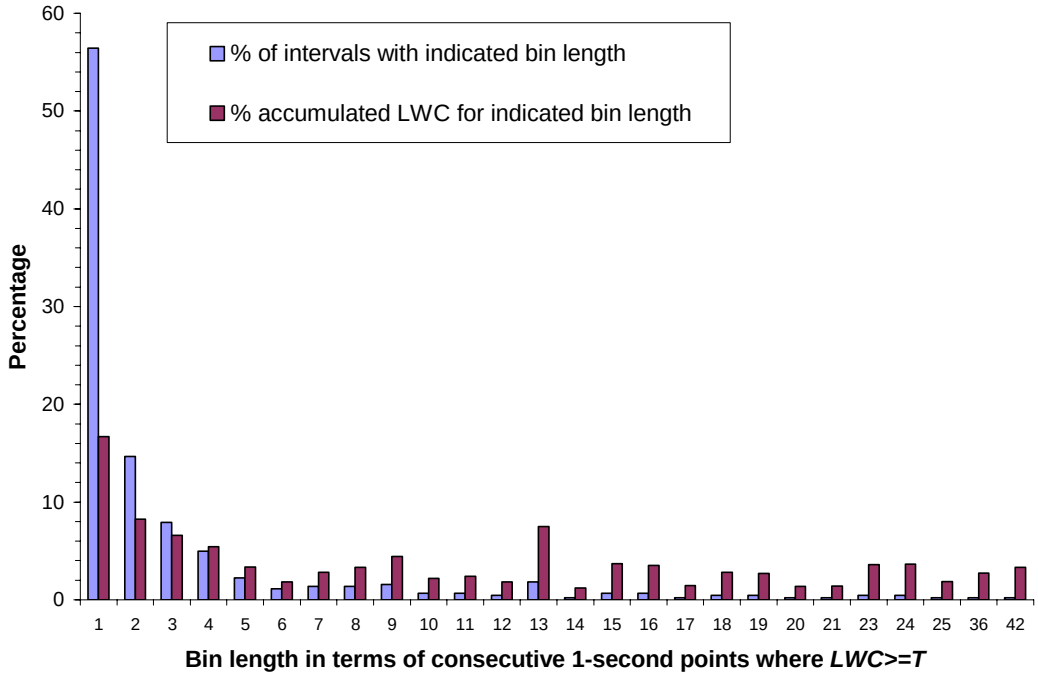

Figure 9b. Percentages of intervals and accumulated LWC by bin length for flight segment 980204f2.

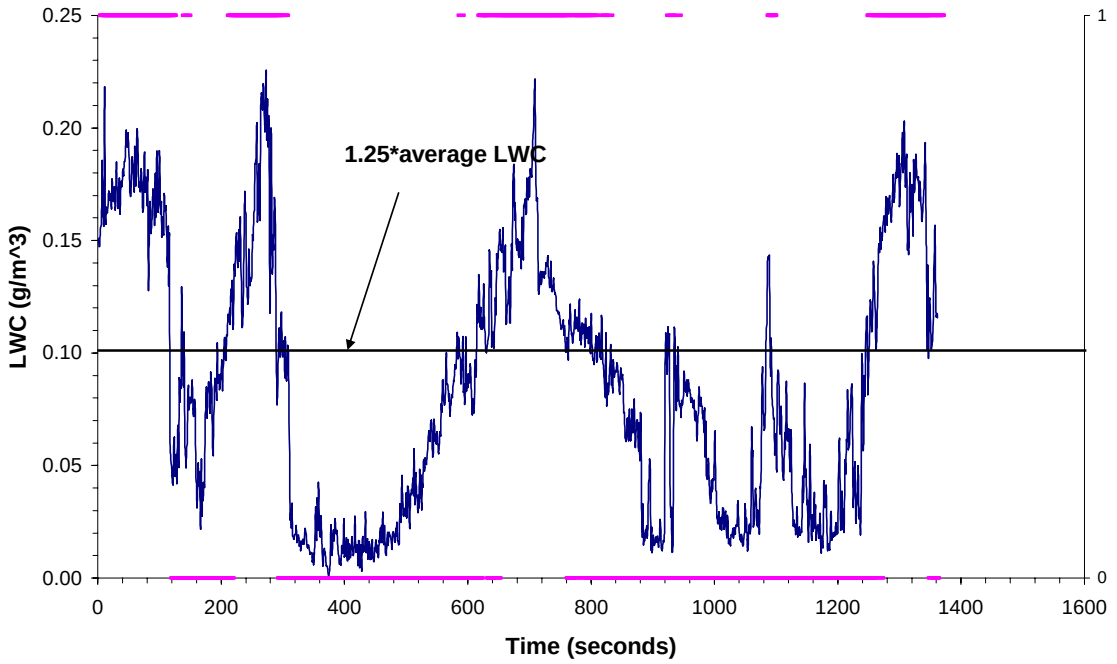

Figure 10a. Magenta lines represent LWC greater or equal to the threshold or less than the threshold for flight segment 980130f1. See text for additional explanation.

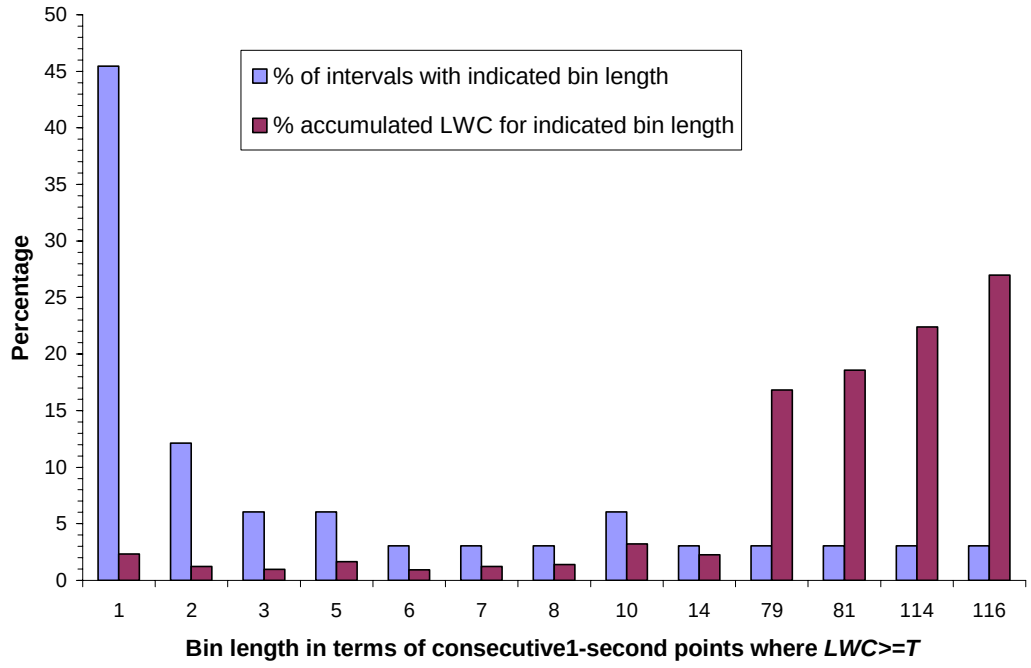

Figure 10b. Percentages of intervals and accumulated LWC by bin length for flight segment 980301f1.

Table 5. Relationships between LWC and MVD, TT, ST, DP, ALT, and FSSP 5-s running means as expressed by r^2 values.

	MVD	TT	ST	DP	ALT	FSSP
980318f1a	0.087	0.085	0.061	0.430	0.193	0.498
980318f1b	0.023	0.011	0.072	0.124	0.082	0.398
980302f1	0.221	0.073	0.070	0.427	0.122	0.669
980227f1	0.507	0.294	0.148	0.019	0.030	0.460
980224f1b	0.021	0.013	0.090	0.470	0.019	0.600
980212f1	0.842	0.159	0.373	0.021	0.007	0,.369
980205f2	0.003	0.027	0.085	0.052	0.198	0.232
980205f1	0.087	0.157	0.145	0.079	0.083	0.164
980204f3	0.312	0.070	0.041	0.061	0.028	0.407
980205f2	0.012	0.514	0.525	0.027	0.051	0.151
980204f1a	0.138	0.255	0.087	0.003	na	0.302
980204f1b	0.050	0.057	0.067	0.081	0.148	0.099
980130f1	0.432	0.168	0.105	0.172	0.275	0.797
980122f1	0.178	0.581	0.069	na	0.020	0.178

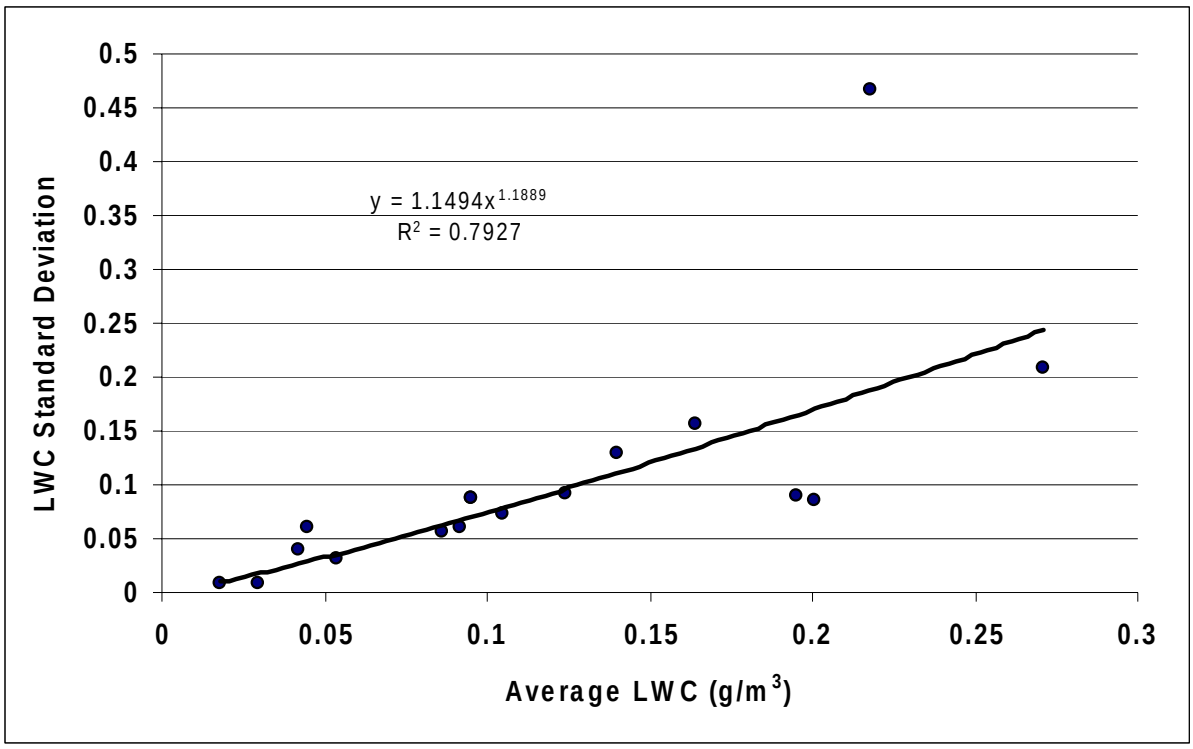

Figure 11. Relationship between average LWC and standard deviation for the 17 flight segements.

relationships with MVD, static temperature, dew point, and altitude. All but one r^2 (with MVD) were less than 0.6 and typically were less than 0.4. Only relationships with FSSP particle concentration were generally high, with all but four being larger than 0.3. A composite correlation for all of the 17 flight segments between LWC and FSSP concentrations yielded an r^2 0.45.

Politovich (1999) demonstrated that there was a relationship between LWC mean and standard deviation in a 106 flight segment database. Our 17 cases from the SLDRP flight segments show a very strong relationship (Figure 11).

6. DISCUSSION

The safety of aircraft in icing conditions is dependent upon the ability of the aircraft to deice or anti-ice in the encountered conditions, which is dependent upon the ability of forecasters to accurately depict the conditions prior to encounter. Aircraft must not fly into conditions predicted to be more severe than the aircraft ice protection systems can tolerate. Two elements are required for prediction; icing intensity (trace, light, etc) and the variability of the supercooled LWC along the path. The second predicted information provides insight on the icing type (rime, clear, etc) when the Ludlum limit is considered.

Our analyses suggest that typical measures of cloud LWC made at 1-s intervals may be used to characterize and predict the variability of LWC. Utilizing clustering techniques, we found that a relationship exists, at least for LWC in three flight segments analyzed, between flight segment global standard deviation and the ratio of cluster segments versus gap segments.

Another approach, based upon threshold techniques indicates that, for our 17 flight segments, there is a general power law relationship between average LWC and flight segment global standard deviation. That is, if average LWC can be measured or predicted then an estimate of LWC standard deviation can be predicted. Such a relationship, if it holds for large geographic regions, or for specific cloud types or synoptic conditions, could be used to create climatologies to improve regional icing forecasts and provide pilots with an indication of hazard potential.

The correlative analysis for the 17 flight segments suggests that relationships between LWC and total temperature, static temperature, dew point, and altitude are quite weak. Only measured or predicted particle concentrations, whether liquid or ice, have any ability to predict cloud liquid water content or vice versa. Politovich (1999) indicates that the variability of LWC may be related to mean LWC, and our SLDRP measurements provide similar results.

7. CONCLUSIONS

The techniques presented in this paper indicate that the ability to predict the variability of LWC from predicted average or cumulative values is promising. In general, variability increases as the mean increases. If acceptable, these techniques could be used to create climatologies of LWC variability with predicted mean LWC based upon region, cloud type, or synoptic environment. All that is necessary is appropriate inflight LWC measurements.

8. ACKNOWLEDGEMENTS

The authors thank the Federal Aviation Administration Aviation Weather Research Program and the National Center for Atmospheric Research Inflight Icing Product Development Team for funding. We also thank the NASA-GRC Icing Branch for providing the SLDRP flight data. The views expressed arethose of the authors and do not necessarily represent the official policy of the FAA.

9. REFERENCES

Jameson, A.R. and A.B. Kostinski, 2000: *The Effect of Stochastic Cloud Structure on the Icing Process. J. Atmos. Sci.,* 55, 2883-289*1*

Koenig, G., C. Ryerson, J. Larsson, and A. Reehorst: 2003, Effect of Variable LWC on Ice Shape in the NASA-GRC IRT. *AIAA-2003-0904, American Institute of Aeronautics and Astronautics 41st Aerospace Sciences Meeting and Exhibit*, 6-9 January, Reno. 11 p.

Kostinski, A.B., and A.R. Jameson, 1997: Fluctuation properties of precipitation. Part I: On deviations of single-size drop counts from the Poisson distribution. *J. Atmos. Sci.***,** *54, 2174-2186*

Miller, D., T. Ratvasky, B. Bernstein, F. McDonough, and J. Strapp: 1998, "NASA/FAA/NCAR Supercooled Large Droplet Icing Flight Research: Summary of Winter 96–97 Flight Operations." *NASA/TM-1998-206620, AIAA-98-0577*, 26 p.

Politovich, M. K., 1999: How can we Use and Depict Variability of Clouds in Icing Forecasts? In *Proceedings of the American Meteorological Society 8th Conference on Aviation, Range, and Aerospace Meteorology*, Dallas, P. 443-446.

Ryerson, C., G. Koenig, R. Melloh, D. Meese, A. Reehorst, and D. Miller, 2001, Spatial Analysis of Great Lakes Regional Icing Cloud Liquid Water Content. *American Institute of*

Aeronautics and Astronautics, AIAA-2001-0394, 11 p.

Ryerson, C., R. Melloh, and G. Koenig, 2002, Clustering of Cold Cloud Microphysical Properties. In *Proceedings of the American Meteorological Society 11th Conference on Cloud Physics*, 3-7 June, Ogden, Utah, paper P2.12 (proceedings not paginated on CD).